BBC

RESEARCH DEPARTMENT

REPORT

An electronically-steerable active receiving array for h.f.

A.P. Robinson, B.Sc., A.R.C.S.
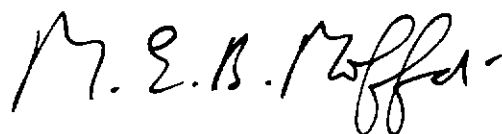
AN ELECTRONICALLY-STEERABLE ACTIVE
RECEIVING-ARRAY FOR H.F.
A.P. Robinson, B.Sc., A.R.C.S.

Summary

The array described offers advantages over the directional aerials commonly used for monitoring at h.f. It is compact and can be steered electronically in any direction. A steerable null may be placed in the radiation pattern. Active elements are used so that the effects of mutual coupling are negligible. The array comprises eight short, vertical monopoles in a line, the outputs of which are passed through variable delay lines, and summed. The system is highly linear and has a large dynamic range. The delay lines comprise nine binary steps and are controlled by a microprocessor to give the desired patterns in response to the control settings. The array has proved a useful addition to the aerial systems at the BBC Monitoring Station.

Issued under the Authority of

M. E. B. Roffed

Head of Research Department

AN ELECTRONICALLY-STEERABLE ACTIVE
RECEIVING-ARRAY FOR H.F.

A.P. Robinson, B.Sc., A.R.C.S.

AN ELECTRONICALLY-STEERABLE ACTIVE
RECEIVING-ARRAY FOR H.F.
A.P. Robinson, B.Sc., A.R.C.S.

1. Introduction

The aerial array has been designed for use by the Monitoring Service in the h.f. band. The aim has been to produce a relatively simple system which nevertheless gives a useful performance. At present, monitoring stations often use passive aerials which tend to be large and either fixed or mechanically steerable. Many fixed aerials are needed if coverage of all the points of the compass is required.

It has been desired for some time to install a different type of receiving-aerial system, because of the benefits which may be obtained. The equipment to be described is the result of a number of development projects.

The advantages of this array are that: it is compact, it can be steered electronically in any direction, and a steerable null can be placed in the radiation pattern*. The steerable null is particularly valuable in view of the congested state of the h.f. broadcast bands. The null could also be used to reduce the effects of an unwanted mode of propagation. Short, active elements are used to simplify the production of the required radiation pattern. The elements are vertical monopoles placed on the ground.

2. Principles of pattern formation

We have arranged the elements in a straight line because this keeps the radiation pattern calculations reasonably simple. Two characteristics of a linear array are that it has greater discrimination between directions in the broadside mode than in the endfire mode, and that (with omni-directional elements) the pattern has mirror symmetry about the line of the array. These are not serious disadvantages in many applications because we can usually place the array broadside to the sector of most interest.

The spacing between the elements needs to be somewhat less than half a wavelength at the highest frequency of operation. We have chosen a spacing of 5 m giving a maximum frequency of about 26 MHz. This covers the highest band allocated for h.f. broadcasting. The lowest frequency of useful operation depends on the aperture of the array. We use

eight elements, so the aperture is 35 m, giving a lower frequency limit of about 6 MHz.

In order to control the radiation pattern of the array, we pass the signals from the elements through variable delay lines and add them together, as shown in outline in Fig. 1. The most straightforward radiation pattern is a steerable main beam. We obtain this by applying a linear delay slope across the array. The calculations are described in Appendix 1. The delays inserted compensate for the propagation delays of a signal arriving from the desired direction, so the signal arrives in phase at the outputs of all the delay lines. This approach has the advantage that the direction of the main beam is independent of frequency. A further advantage of using delay lines rather than phase shifters is that they are much easier to construct, particularly in a passive form; if active devices were used in the phase shifters the non-linearity might cause difficulties when receiving weak signals in the presence of strong ones.

For any main-beam direction, the output voltage of the array is eight times that which would be obtained if only one element was connected. An example of a calculated pattern is shown in Fig. 2, for a frequency of 12 MHz with the main beam steered to $+20°$ relative to broadside. The "simulated" pattern is obtained by a method discussed later (see Section 5.2).

We can also produce a radiation pattern with a steerable main beam and a steerable null. We have
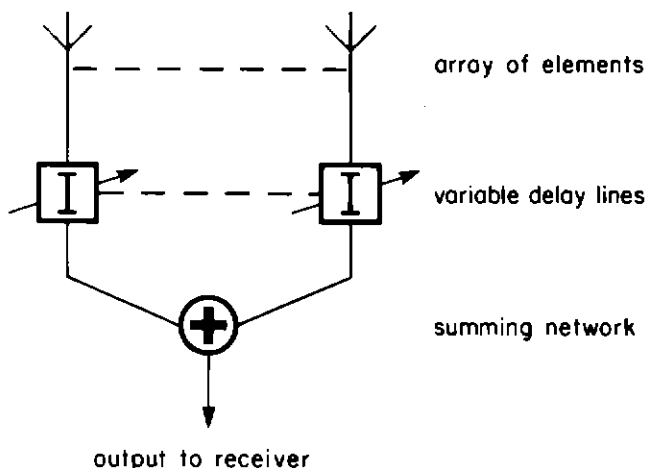

output to receiver

Fig. 1 – Principle of steerable array.

---

*It is convenient to use the term "radiation pattern" although we are considering an array which only receives.
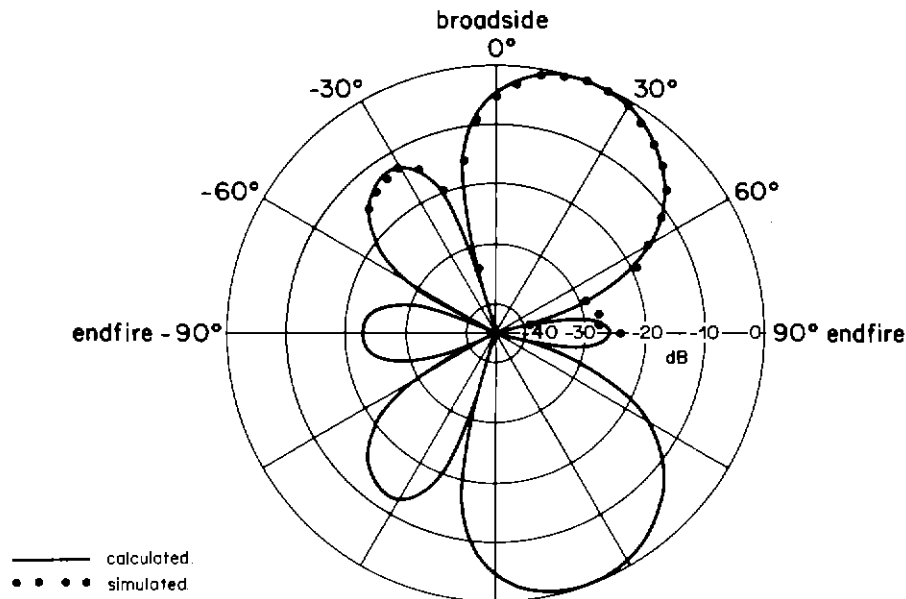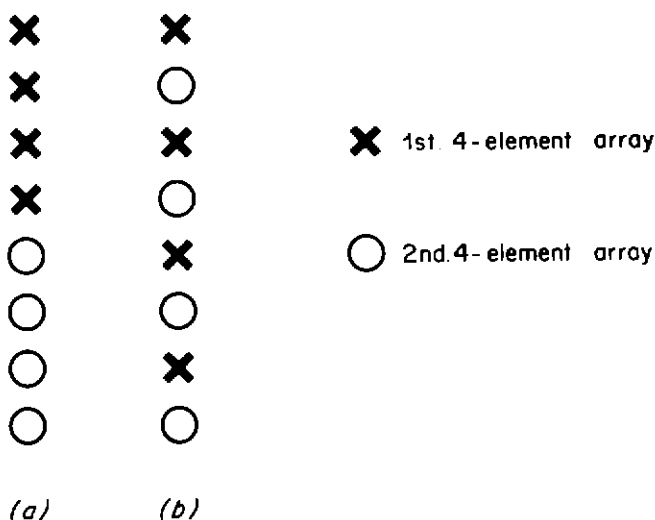
Fig. 2 – Calculated and simulated patterns at 12 MHz with main beam steered to + 20° relative to broadside.

adopted a simple method which only requires adjustment of the delay lines. This avoids the additional difficulties associated with variable attenuators or gain stages, which would have to be highly linear.

The null-forming strategy uses the principle of the multiplication of patterns. Fig. 3 shows two ways of splitting the array into two four-element arrays, (a) by dividing it in the middle and (b) by assigning alternate elements to each sub-array. The main beam of each four-element array is steered in the wanted direction. A check is made for both configurations of the array, that the four-element pattern

does not contain an additional main lobe. (Details are given in Appendix 1.) Then a phase difference is applied between the four-element arrays to place the null as required. Figs. 4 and 5 show the resulting patterns for the two configurations at 12 MHz with the wanted signal at +20° (as in Fig. 2), and a broadside null. A check is made that the sensitivity of the array in the wanted direction has not been reduced by more than 6 dB. This represents a reasonable compromise between allowing a useful range of null positions and preventing gross distortion of the main beam. The pattern of Fig. 5 fails this check.

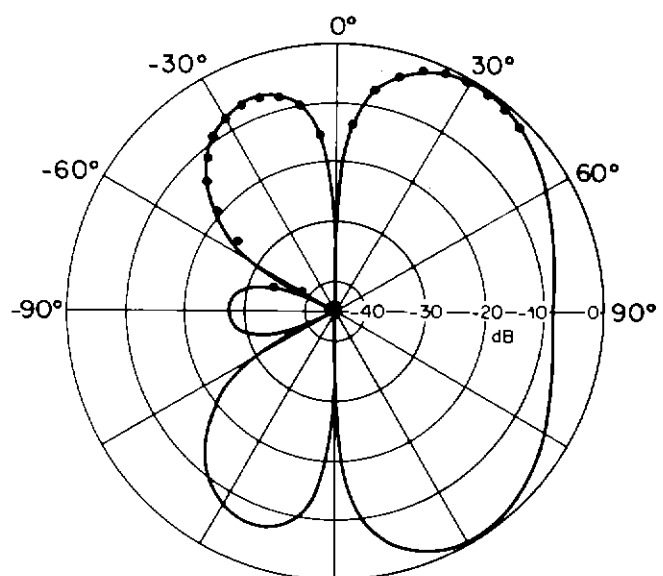*Fig. 3 – Two configurations of the array for null steering.*

Fig. 4 – Calculated and simulated patterns at 12 MHz. Wanted signal at +20° and null at 0° with configuration of Fig. 3(a).

If both configurations pass all the checks, the one giving the greater sensitivity in the wanted direction is chosen. If both fail, we fall back to the steerable main beam, and displace the whole pattern by up to half the width of the appropriate sidelobe or a quarter of the width of the main lobe in order to place the null. As a result the sensitivity in the wanted direction may be reduced by up to 4 dB. Fig. 6 shows what the fall-back pattern would be for the example we have been following. The pattern has been displaced by almost the maximum amount we allow.

In fact, with the wanted signal at $+20°$, configuration (a) permits us to steer the null up to $+5°$ from broadside before the pattern fails the checks. If the null direction called for is too close to the main beam, we cannot produce the null, and the array control system would indicate this.

Since this work was completed, attention has been drawn to an improved procedure for null steering again by adjustment only of phases[1] which might be used in future. A description of the method is given in Appendix 2.

3. System description

A block diagram of the complete equipment is shown in Fig. 7. The array itself comprises eight active vertical monopoles arranged in a line (see Fig. 8). The signals from the elements pass through a set of variable delay lines and are then added together to give the output for a receiver. The system for controlling the delay lines is built around a
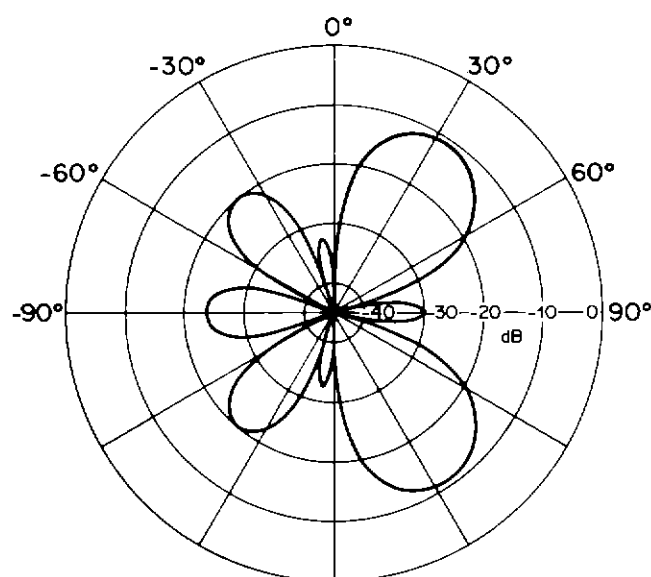
microprocessor. The main beam and optional null can be steered by means of control knobs or thumb-wheel switches (see Fig. 9). A serial data link is provided so that the array may be controlled remotely, via an audio line.

3.1. Performance parameters derived from theory

Frequency range: 6 MHz to 26.1 MHz.

Half-power beamwidth at low elevation angle (without steerable null):

| | main beam direction | | |
frequency	broadside (2 beams)	30° from broadside* (2 beams)	endfire (1 beam)
6 MHz	68°	93° (+33° to −60°)†	127°
11 MHz	35°	43° (+19° to −24°)	92°
16 MHz	24°	28° (+13° to −15°)	75°
21 MHz	18°	21° (+10° to −11°)	66°
26 MHz	15°	17° (+8° to −9°)	59°

*Figures in brackets indicate actual angles with respect to main beam maximum. "+" indicates towards the broadside direction and "−" indicates towards the endfire direction.

†One of the endfire directions is within the half-power beamwidth so that the two beams are contiguous.

Peak sidelobe level (without steerable null): 13 dB below main beam.

Minimum angle between null and main beam:
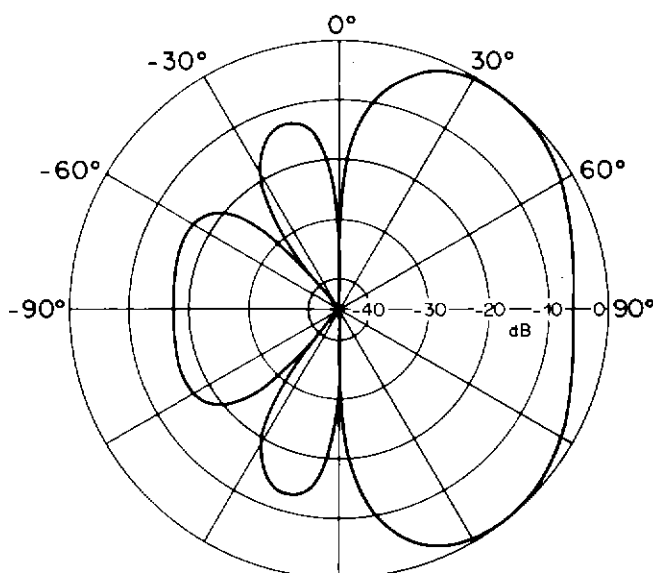

Fig. 6 – Calculated pattern at 12 MHz for fall-back strategy. Wanted signal at $+20°$, main beam steered slightly off to give null at 0°.

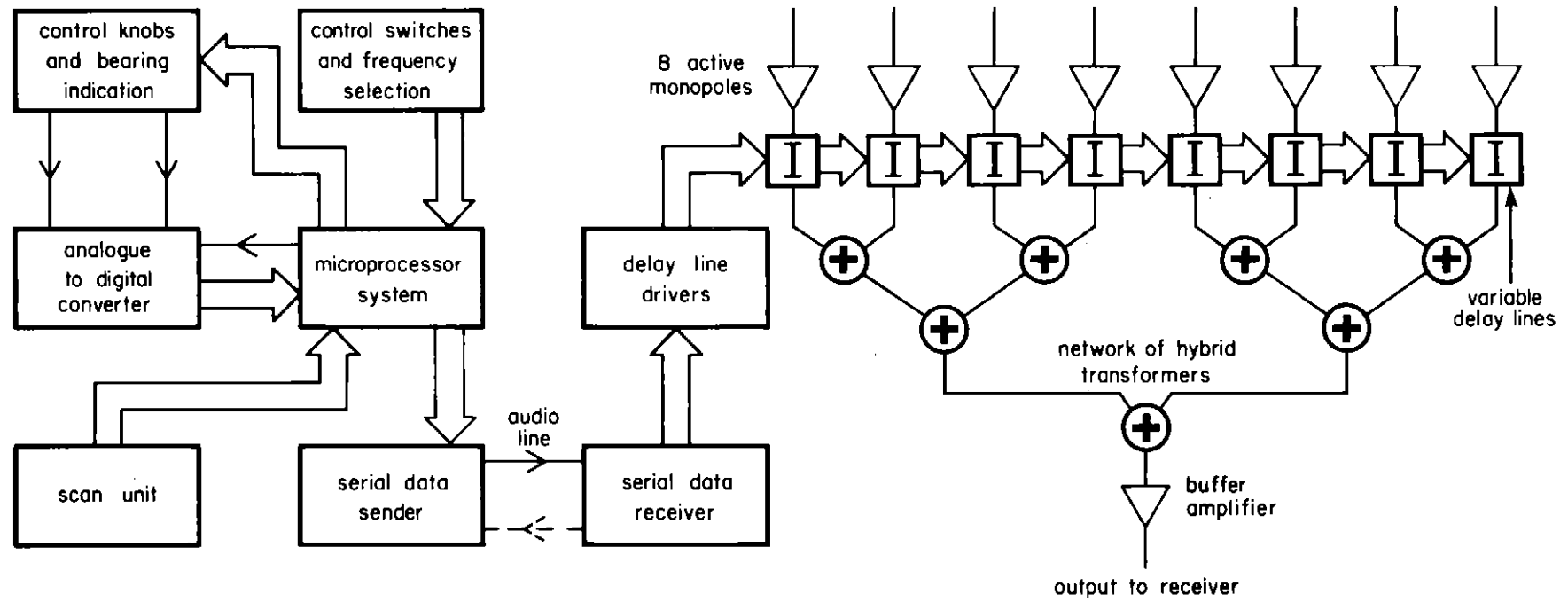Fig. 5 – As Fig. 4 but with configuration of Fig. 3(b).

Fig. 7 – Block diagram of steerable array.

Fig. 8 – The array of eight active monopoles.

| frequency | main beam direction | | |
	broadside	30° from broadside	endfire*
6 MHz	25°	+25°, −37°	55°
11 MHz	14°	+15°, −17°	41°
16 MHz	10°	+10°, −11°	34°
21 MHz	7°	+8°, −8°	30°
26 MHz	6°	+6°, −7°	37°

* In some cases application of the null increases the delay slope beyond that required for endfire and this reduces the beamwidth.

Loss of sensitivity in main beam direction when null is switched on: Less than 6 dB.

3.2. Performance parameters derived from measurement*

Sensitivity in main beam direction: approximately 0.5 V into 50 ohm load for 1 V/m field strength, nearly independent of direction and frequency.

Output impedance: Low (< 20 ohms).

Radiation patterns: see Section 7.1

Null depth in direction selected: Normally better than 20 dB below main beam, typically better than 25 dB down. (Deepest point of null may be slightly away from direction selected.)

Noise performance: The noise power due to internal noise sources, delivered into a 50 ohm load, varies from about 21 dB at 6 MHz to about 14 dB at 26 MHz, relative to thermal noise. The noise power received from external sources will be greater than this in many environments. As a guide, the level of man-made noise which would contribute a noise power at the array output equal to that due to internal noise sources corresponds approximately to CCIR Report 258–4, Fig. 1, curve C ("rural area")[2]. This calculation has made certain assumptions about the man-made noise. Other external sources of noise may also be significant.

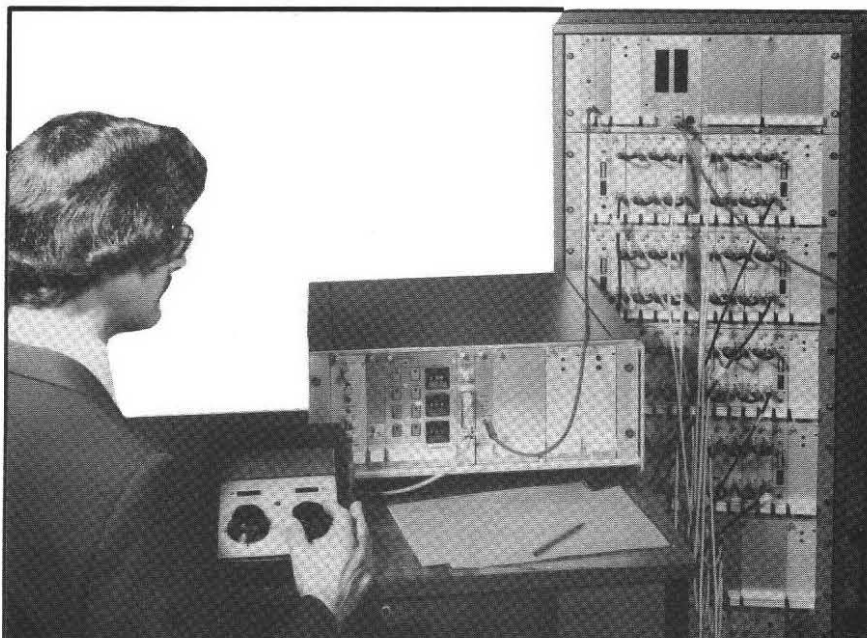*With 100 m PSF1/2M cable between each element and the combining bay.

Fig. 9 – The operator's control position with the combining bay in the background.

Intermodulation performance: With two un-wanted signals each of 250 mV/m field strength the second- and third-order intermodulation products are better than 90 dB down, i.e. less than 8 μV/m equivalent field strength.

3.3. Design parameters

Control of main beam and null directions: by control knobs (continuous 360° rotation corresponding to points of compass) or thumb-wheel switches. The main beam is steered to the nearest 5° and the null to 256 positions around the compass. The control system can easily be reprogrammed for different orientations of the array.

Serial data signal: In accordance with RS-232C; 7 bits plus start and stop bits. Link-selectable speeds 19200, 9600 and 4800 baud.

4. The active element

The element is a 2 m vertical whip with a high-input-impedance amplifier at its base[3]. This ensures that the current flowing in the whip is small so that re-radiation is negligible and mutual coupling effects between elements can be ignored. Hence it is straightforward to calculate the radiation pattern of the array. The element is designed to operate over the frequency range 150 kHz to 30 MHz.

We have imposed stringent requirements for linearity and signal handling upon the array because we may wish to receive a weak signal in the presence of a very strong one. (This could occur if the array is used near a transmitting site, for example, as a re-broadcast receiving array.) Care was therefore taken in the design of the amplifier used in the elements.

The linearity controls of the amplifier were initially adjusted for optimum performance at one frequency with a low impedance source[3]. After minor modifications we obtained good performance over the h.f. band with a source impedance which simulated the whip as well as with lower impedances. We used a two-tone test to check the linearity; with care, very low levels of distortion can be measured. At an input level of 200 mV for each signal (*i.e.* 1.1 V peak to peak), the second- and third-order inter-modulation products measured at the output of the amplifier were better than 90 dB down, that is, less than 6.5 μV equivalent at the input.

Incorporated in the amplifier is a network to feed a "contact wetting" current through the output connector and down the cable (see Section 5.1).

The amplifier is housed in an aluminium box at the base of the whip. Attention has been paid to sealing the box to withstand the changes in internal pressure which are caused by temperature vari-ations, so that moisture will not be drawn in. The whip itself is supported by a fibreglass tube. The element is mounted on a sheet of galvanised steel mesh 2.4 m by 1.2 m which acts as an earth plane. These features can be seen in Fig. 8 which shows the array of eight elements.

5. The combining equipment

The combining equipment is completely passive in order to give good linearity, except that there is a buffer amplifier at the output, which is similar to the amplifier just described.

5.1. Delay lines

The combining bay contains eight variable delay lines, plus a spare. Each delay line is made up of nine steps in a binary sequence, from $\frac{1}{4}$ ns to 64 ns, so we can obtain any delay in $\frac{1}{4}$ ns steps up to $127\frac{3}{4}$ ns. For the 5 m element spacing chosen, this total is slightly greater than the propagation time between the first and last elements of the array. The smallest delay step of $\frac{1}{4}$ ns gives an azimuthal resolution, for a pair of adjacent elements, of better than two degrees over three-quarters of the circle of directions. Fig. 10 shows two of the delay cards. The delays up to 16 ns are made of microstrip lines; the 32 ns and 64 ns delays are lengths of miniature coaxial cable.
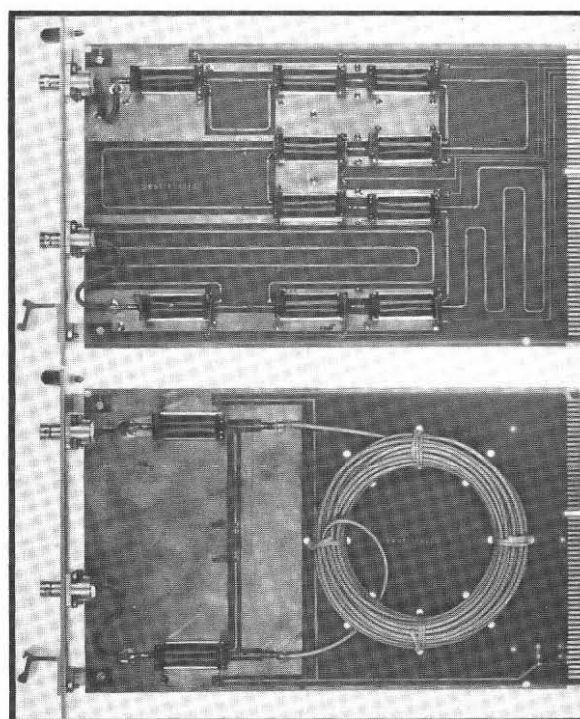

Fig. 10 – Microstrip and cable delays.

The delays are switched in and out by change-over reed relays. Reed relays were chosen because they would not be a source of non-linearity. They also give low insertion loss when closed and good isolation when open (which prevents ripples in the amplitude- and delay-frequency responses arising from coupling to an unselected path). The switching time of the reeds we use is about 2 ms. This is not a significant limitation on the speed at which we adjust the delay lines.

The wetting current fed in from each element amplifier flows through all the reed contacts. A d.c. of 2 mA is used; this prevents an early increase in the contact resistance and greatly extends the life of the reeds. The delays have a 75 ohm characteristic impedance because we were able to obtain a good match of the reeds to this impedance. Each reed is mounted in a coaxial brass tube connected to earth. Fig. 11 shows the trace obtained on a time-domain reflectometer from a reed switch, aligned with a diagram of the reed switch arrangement. The displayed reflection coefficient is within ±7%. At frequencies up to 26 MHz, however, the effective reflection coefficient of the switch is considerably less.

The length of each delay was measured in terms of its phase shift at a known frequency. The errors in the individual delays, and the overall error with the nine delays in tandem, are all within about $\pm\frac{1}{4}$ns. When connecting the delays in tandem, we noted small additional delay errors, due to slight variations in the characteristic impedance.

5.2. Interconnection and checking performance

It is also necessary that the interconnecting cables between the elements and the combining bay do not introduce significant delay differences. To keep the errors in the electrical length to within $\pm\frac{1}{8}$ns the cable lengths must be cut to an accuracy of ±25 mm. The cables in use at present are 100 m long.

The main imperfection in the combining equipment arises from attenuation in the delay lines. Compensating attenuators have been placed in the bypass paths for the three longest delay steps, but exact compensation is only obtained at one frequency. Fig. 12 shows the frequency response of a variable delay line for four delay settings which give extremes of attenuation. At some frequencies, the insertion loss can vary over a 1 dB range as the delay is changed, although typical variation is 0.6 dB.

The signals from the delay lines are summed in a network of hybrid transformers. The performance of the transformers is very good in all respects. The buffer amplifier at the output ensures that the network is correctly terminated, irrespective of the load presented by a receiver.

The length of each delay line is controlled by a delay-line driver unit. The unit supplies the current to operate the reed relays and indicates the present length of the delay line. The unit stores the delay setting in latches which can be loaded either by switches on the front panel or remotely by the array
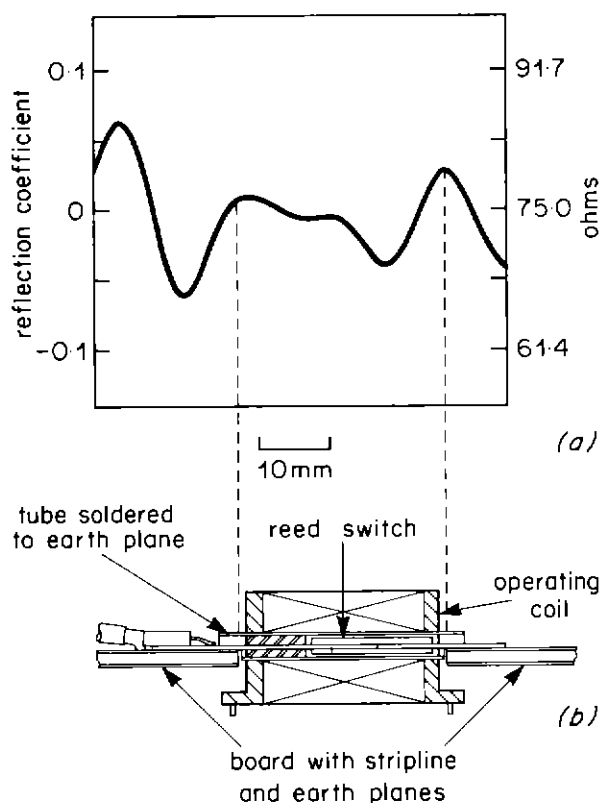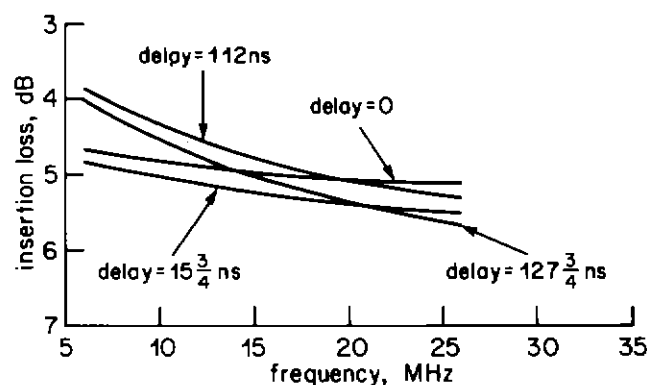

Fig. 11 — (a) Trace obtained on time-domain reflectometer from reed switch (b) Cross-sectional view of reed switch, showing relationship to trace.

Fig. 12 — Insertion loss of variable delay line.

control system. Fig. 13 is a photograph of the combining bay and it may be noted that no attempt has been made to minimise the space occupied by the equipment, but the simple modular arrangement aids servicing.

We tested the combiner as a whole by feeding equal in-phase signals into the eight inputs. We scanned the delay settings round from endfire one way to endfire the other way, in five degree steps, measuring the combiner output. Fig. 14 shows the result at 15 MHz compared with calculation and it may be seen that there was good agreement. We have
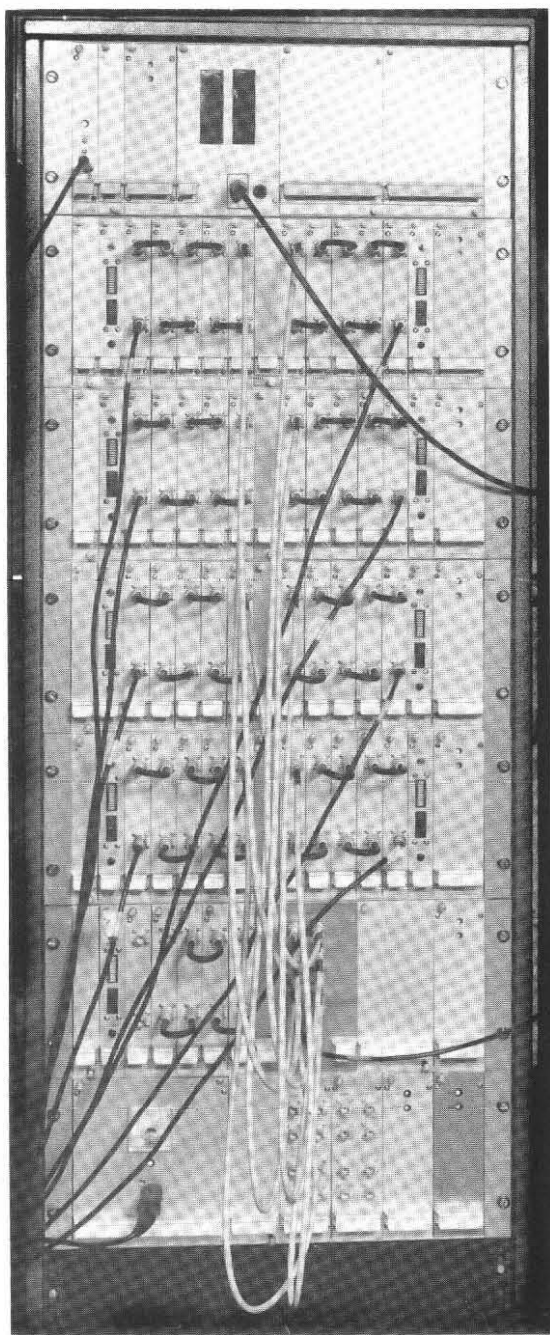

Fig. 13 – Combining bay.

simulated a broadside pattern because, for example, the delays inserted for the one endfire direction are equal to the propagation path delays for a signal arriving from the other endfire direction.

The simulation can be extended to any pattern: in each signal path, we insert in addition the delay required to produce the particular pattern. Consequently for some patterns there is not enough delay available to simulate all the directions. We simulated the patterns of Figs. 2 and 4 and the results plotted show good agreement with calculation.

The nulls we obtain in this simulation are usually more than 30 dB down on the main beam. The null depth is limited by errors in the combiner, and by the quantisation of delays and directions. The performance in this respect is quite satisfactory for the present application.

6. Control system

The control system is shown in the block diagram, Fig. 7. The control system is built around a microprocessor. A microprocessor is a suitable device to carry out a moderately complicated procedure, such as forming patterns as described earlier, where the burden of calculations is not too great. It is also quite easy to interface peripheral devices to a microprocessor.

There is a small control box for the operator of the array. The box, shown in Fig. 15, incorporates knobs for steering the main beam and null directions, and numerical displays for the two directions in degrees. A light marked "setting invalid" indicates, for example, when a null cannot be produced.

Apart from the knob control box, the control system is housed in a standard rack. Fig. 16 depicts the control rack. On the front panel, there are pushbuttons to select the mode of operation of the array. There are also thumbwheel switches for setting the frequency if the steerable null is being used, and for steering the array, as an alternative to the knobs.

A scan unit is provided which swings the main beam rapidly through 180° in 5° steps. The scan speed is variable. A display of signal strength against direction can thus be produced by the use of a suitable receiver and display device. This is useful for direction finding. The arrangement will also display a simulated broadside pattern (see Section 5.2). An additional facility allows any pattern to be simulated, the display or plot being swept out by the scan unit. The simulated patterns are useful when testing because it is immediately apparent whether the
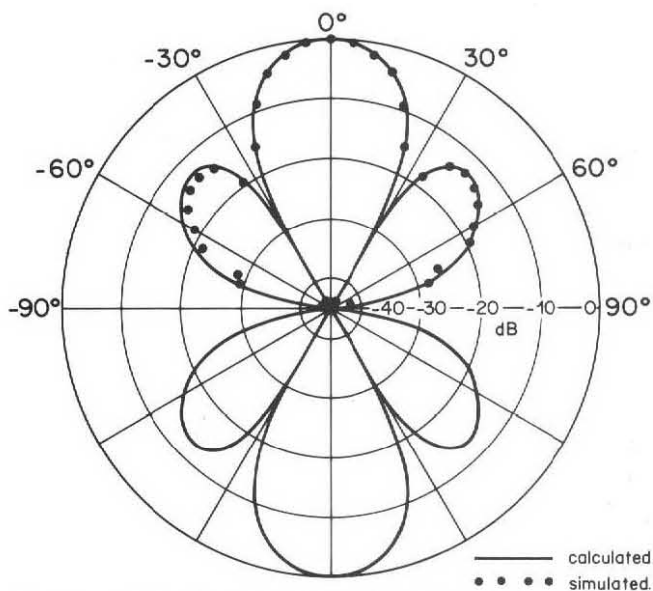
Fig. 14 – Calculated and simulated broadside patterns at 15 MHz.

— calculated
• • • • simulated

Fig. 15 – Knob control box.

software and combining equipment are operating correctly.

The microprocessor produces the delay data in parallel form and can operate the delay-line drivers directly. The combiner can also be operated remotely via an audio line. In this case a serial data sender and receiver are interposed. It takes $7\frac{1}{2}$ ms to set all the variable delay lines at the fastest signalling speed we have provided (when the serial data link is in use it is not possible to scan at full speed). The eight delay values come out of the microprocessor in a burst and are stored in the serial data sender until they can be transmitted. The advantage of remote control is that the combiner can be placed near to the array. We thus avoid the need for eight matched

lengths of low loss feeder from the receiving site to the vicinity of the operator's controls. The receiver can either be installed with the combining bay and also be remotely controlled or it can be at the remote operator's position, fed by a single low-loss feeder.

The length of line which can be used to carry the serial data is limited by the required signalling speed and the permissible current which can be injected into the line, but lengths in excess of 200 m are
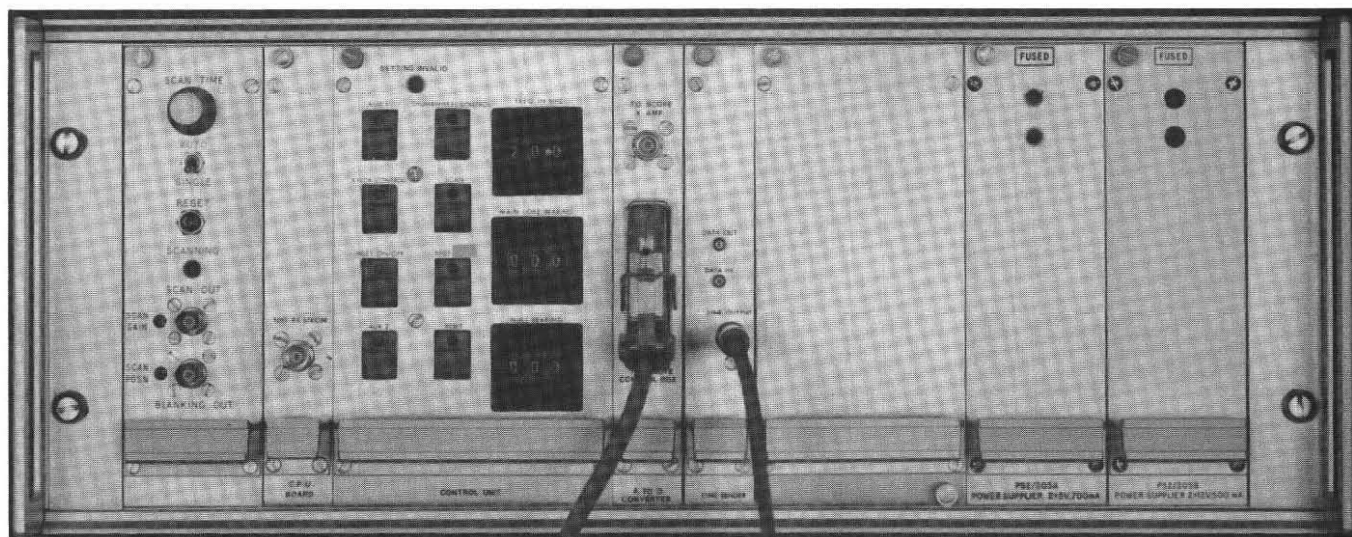

Fig. 16 – Control rack.

possible. Modems could be used for control over longer distances, though the signalling speed may be reduced.

The microprocessor program was written in assembly language. It takes a maximum of 10 ms to read the various controls and do the radiation pattern calculations. The printed listing of the program runs to about fifty pages and the assembled code occupies some 3500 bytes.

7.   Overall performance

7.1. Comparison of theoretical and measured radiation patterns

Since the array only receives, and is too large to be placed on our turntable, we measured the radiation pattern by moving a test transmitter around the array. Relying on symmetry, we need only move the transmitter around a quadrant. The second quadrant of each pattern is obtained by applying the delay values in reverse order along the array. The pattern in the last two quadrants is a mirror image of the first two.

We made pattern measurements with the array installed in the grounds of the BBC Research Department, and also at the BBC Monitoring Station. We marked out nineteen transmitter positions in a quadrant around the array, at five degree intervals from endfire to broadside. The distance from the transmitter to the centre of the array was 100 m at Research Department and 150 m at the Monitoring Station.

We used a receiver which gave the signal strength in digital form in decibels relative to an arbitrary zero. To automate the measurement of patterns, a special facility was added to the microprocessor program. Thus it was possible to measure sixteen patterns at each of five frequencies while the transmitter was placed only once at each of the marked positions.

Examples of radiation patterns are shown in Figs. 17–22. Calculated patterns are given for comparison. The calculated patterns have been obtained using the actual delay values computed by the microprocessor. The effects of having the transmitter quite close have also been taken into account, although it has been assumed that only the radiation component of the field is significant at the distances involved.

The patterns in Figs. 17 and 18 were measured at the Monitoring Station. Figs 19–22 were measured at Research Department. Some distortion is evident in the measured patterns. For the patterns measured at Research Department, the distortion may be ascribed, at least in part, to the somewhat adverse environment: there are trees, huts and other clutter in the grounds, and also underground conductors. Nevertheless, the results show that the far-field null depth would generally be better than 20 dB below the main beam. This indicates that the array is not unduly sensitive to its surroundings and local propagation effects need not be of great concern. On a good site, a typical null depth of 25 dB may be expected, although for sky wave signals this figure
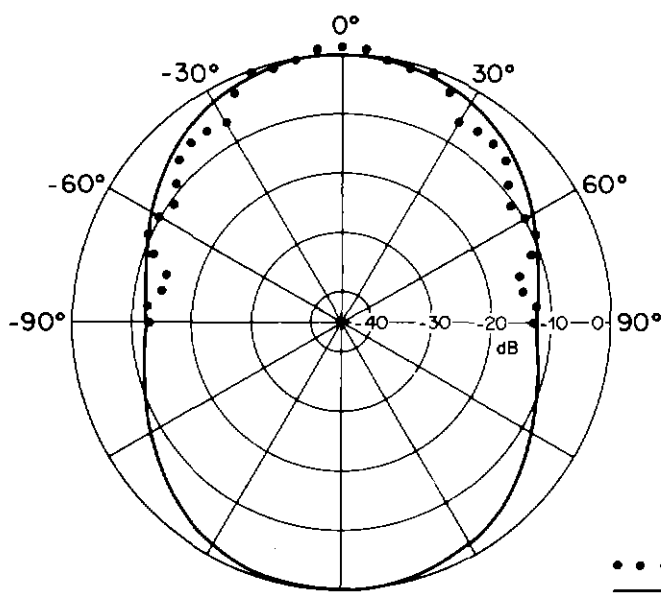

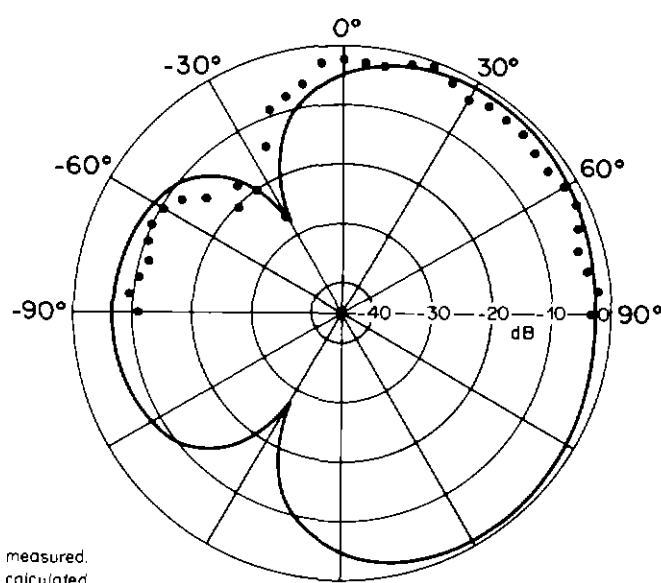*Fig. 17 – Measured and calculated broadside patterns at 6 MHz.*

Fig. 18 – Measured and calculated patterns at 6 MHz. Wanted signal at 0° and null at −30°.
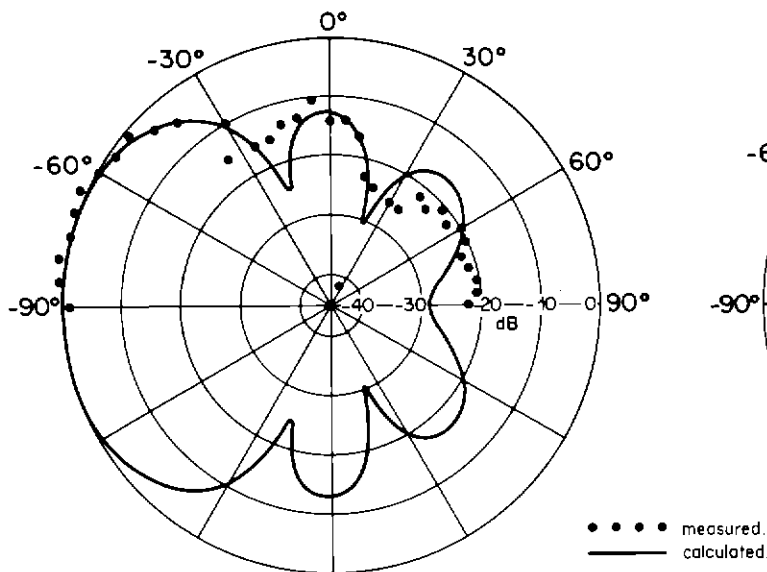
Fig. 19 – Measured and calculated endfire patterns at 11 MHz.

Fig. 21 – Measured and calculated patterns at 21 MHz with main beam steered to −30° relative to broadside.

may be reduced because of irregularities in the ionosphere.

7.2. Operational appraisal

The array is now in operation at the BBC Monitoring Station at Caversham. The users of the array report that its directional properties have proved valuable. On a number of occasions, a signal has not been usable owing to co-channel interference, when received on any of the other aerial systems available, whilst the active array successfully produced a readable signal, by application of the steerable null.

It was also found that weak signals can be received without difficulty. It has been noted, however, that the apparent direction of arrival of sky-wave interference can show small random variations which necessitate frequent adjustment of the null direction control. Switching transients can be distracting when fine adjustments are being made to the null direction, and this aspect may be improved in future equipment.

8. Conclusions

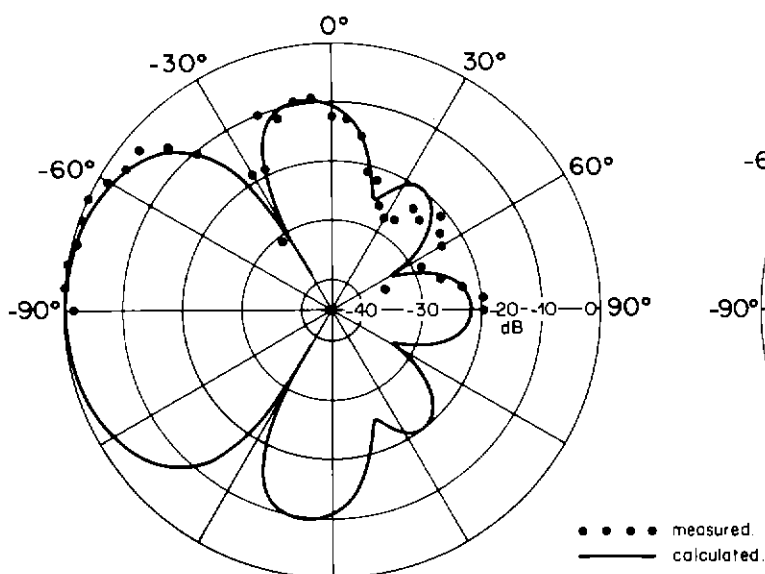Operational experience of the array is encouraging. The steerable null gives a useful ad-

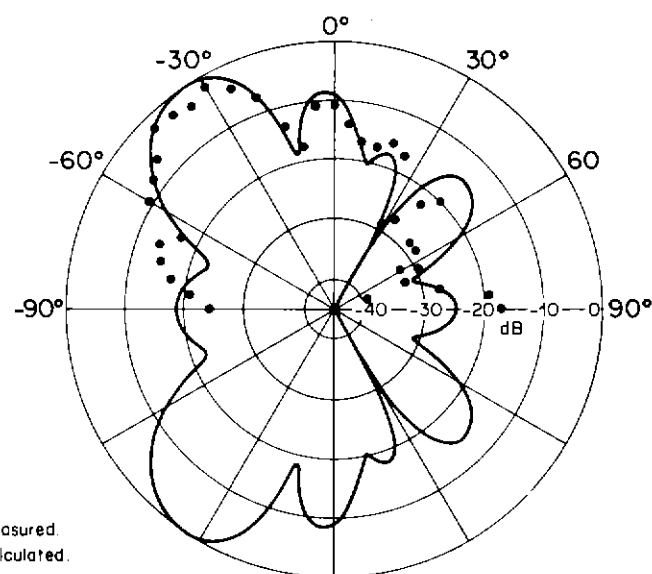*Fig. 20 – Measured and calculated patterns at 11 MHz. Wanted signal at −90° and null at −30°.*

Fig. 22 – Measured and calculated patterns at 21 MHz. Wanted signal at −30° and null at +30°.

ditional degree of freedom to improve the reception of signals when there is interference. Propagation effects are a limitation, which reduce the null depth which can be achieved. There is some advantage in placing the array on a good site though this is not critical.

The use of a microprocessor in the control system has given a number of benefits. The array is easy to operate, and it has been possible to include features such as scanning and test facilities. Modifications and additions can also be made more readily.

9. References

1. ANANASSO, F., 1981. Nulling performance of null-steering arrays with digital phase-only weights. *Electron. Letters* 1981, **17**, 7, pp. 255–257.

2. C.C.I.R., 1982. Man-made radio noise. Recommendations and Reports of the CCIR, Geneva, 1982, **VI**, Report 258–4.

3. LYNER, A.G. *and* PRICE, H.M., 1977. An active aerial element for h.f./m.f. receiving arrays. BBC Research Department Report No. 1977/36.

APPENDIX 1: CALCULATION OF DELAYS TO GIVE DESIRED RADIATION PATTERN

List of symbols

λ wavelength

f frequency

d spacing of elements

d_r spacing of elements in radians $= \dfrac{2\pi d}{\lambda}$

ϕ bearing in radians measured clockwise from broadside (see Fig. 23)

τ delay inserted in path of signal from element $m + 1$ relative to element m (if τ is negative there is more delay in the path from element m)

δ phase equivalent of τ, in radians: $\delta = -2\pi f\tau$

ψ phase in radians of signal from element $m + 1$ relative to signal from element m for a distant source on bearing ϕ, at the point where the signals are combined, *i.e.* including both the propagation path difference and the effect of τ

ϕ_1 bearing on which maximum is required

ϕ_0 null direction(s)

n number of elements

From Figs. 1 and 23, with the same value of τ for each pair of adjacent elements, and with the source in the plane of the diagram

$$\psi = d_r \sin \phi + \delta$$

Taking phases relative to the centre of the array and with unit amplitude for each element, the pattern in the
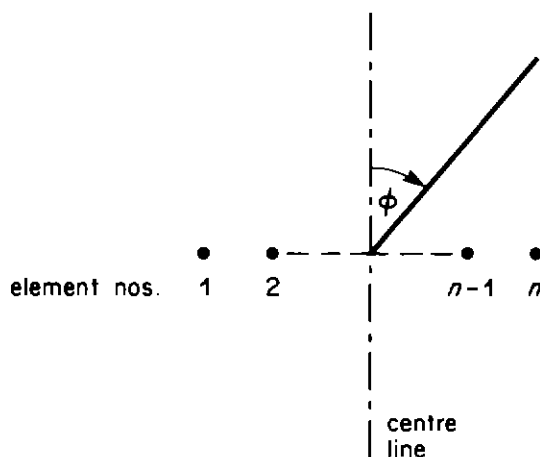

Fig. 23 – Geometry of array.

plane of the diagram is

$$E_n(\phi, d_r, \delta) = e^{j(-n/2+1/2)\psi} + e^{j(-n/2+3/2)\psi} + \ldots + e^{j(n/2-3/2)\psi} + e^{j(n/2-1/2)\psi}$$

$$= e^{j(-n/2+1/2)\psi}\frac{e^{jn\psi} - 1}{e^{j\psi} - 1}$$

(sum of geometric progression)

$$= \frac{e^{jn\psi/2} - e^{-jn\psi/2}}{e^{j\psi/2} - e^{-j\psi/2}}$$

$$= \frac{\sin(n\psi/2)}{\sin(\psi/2)}$$

(The elements are omni-directional in the plane of the diagram. Mutual coupling has been neglected.)

The pattern E_n is plotted as a function of the phase parameter ψ in Figs. 24(a), (b) and (c) for $n = 2, 4$ and 8 respectively. The principal maximum occurs when $\psi = 0$, provided the range of values -1 to 1 for $\sin \phi$ takes ψ to this value. The first sidelobe is about $13\,\mathrm{dB}$ down which is typical for a linear array with equal amplitudes
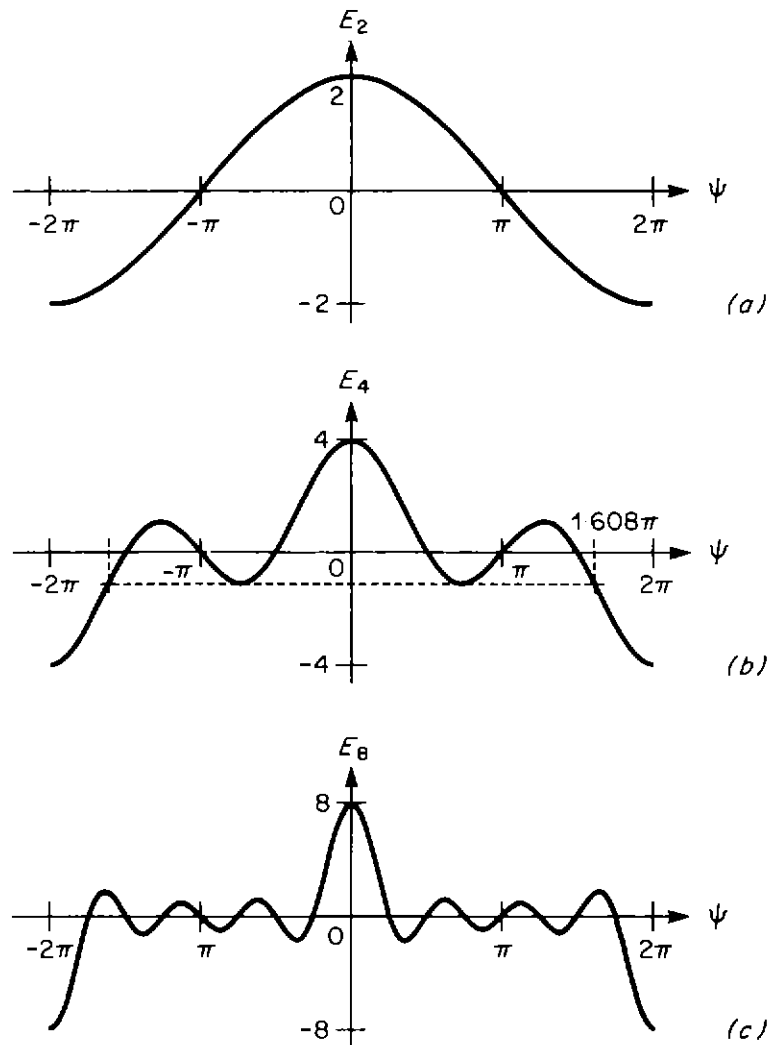

Fig. 24 – Radiation pattern of array, $E_n(\psi)$ (a) $n = 2$ (b) $n = 4$ (c) $n = 8$.

and equal spacing. Given ϕ_1, the bearing of the maximum, we can find the value of τ required to steer the array:

$$0 = d_r \sin \phi_1 + \delta$$

$$\delta = -\frac{2\pi d}{\lambda} \sin \phi_1$$

$$\tau = \frac{d}{f\lambda} \sin \phi_1$$

This shows that the main beam direction is independent of frequency, because $f\lambda$ = speed of light. The appearance of additional, equal maxima in the pattern, corresponding to $\psi = \pm 2k\pi$ ($k = 1, 2, 3, \ldots$), is prevented by choosing $d < \lambda/2$.

We have only considered signals arriving with a zero elevation angle. However, a signal with a typical angle of elevation will appear like a zero elevation signal of slightly different azimuth. Thus the array will operate quite satisfactorily for sky-wave signals, because the exact control setting is only of concern for logging purposes. In fact the radiation pattern in three dimensions is of conical form. The axis is the line of the array and the angle between the axis and the main beam depends on the value of the delay slope. The vertical radiation pattern of the elements is also a factor in the pattern of the array.

The null is produced by the principle of multiplication of patterns. In the following, the left-hand column refers to configuration (a) of Fig. 3 and the right-hand column refers to configuration (b).
The four-element array pattern is

$$E_{4a} = \frac{\sin(4\psi_{4a}/2)}{\sin(\psi_{4a}/2)} \qquad\qquad E_{4b} = \frac{\sin(4\psi_{4b}/2)}{\sin(\psi_{4b}/2)}$$

where $\psi_{4a} = d_r \sin \phi + \delta_{4a}$ where $\psi_{4b} = 2d_r \sin \phi + \delta_{4b}$

(The ψ's and δ's refer to phase differences between successive elements of the sub-array in question, or between the two sub-arrays; d_r is the same as above.)

The two-element (array of arrays) pattern is

$$E_{2a} = \frac{\sin(2\psi_{2a}/2)}{\sin(\psi_{2a}/2)} \qquad\qquad E_{2b} = \frac{\sin(2\psi_{2b}/2)}{\sin(\psi_{2b}/2)}$$

$$= 2\cos(\psi_{2a}/2) \qquad\qquad = 2\cos(\psi_{2b}/2)$$

where $\psi_{2a} = 4d_r \sin \phi + \delta_{2a}$ where $\psi_{2b} = d_r \sin \phi + \delta_{2b}$

The null occurs when $\psi_{2a}/2$ or $\psi_{2b}/2 = \pm\frac{\pi}{2}, \pm\frac{3\pi}{2}, \ldots$

The resulting eight-element pattern is

$$E_a = E_{4a}E_{2a} \qquad\qquad E_b = E_{4b}E_{2b}$$

To steer the main beam of the four-element pattern in the direction ϕ_1

$$0 = d_r \sin \phi_1 + \delta_{4a} \qquad\qquad 0 = 2d_r \sin \phi_1 + \delta_{4b}$$
$$\delta_{4a} = -d_r \sin \phi_1 \qquad\qquad \delta_{4b} = -2d_r \sin \phi_1$$

Substituting,

$$\psi_{4a} = d_r(\sin \phi - \sin \phi_1) \qquad\qquad \psi_{4b} = 2d_r(\sin \phi - \sin \phi_1)$$

To avoid an additional main lobe we must restrict ψ (see Fig. 24(b))

$$|\psi| \leqslant 1.608\pi$$

The extreme value of ψ occurs in one of the endfire directions, *i.e.* when $\sin \phi = \pm 1$. Thus the condition for success of the configuration is

$$d_r(1 + |\sin \phi_1|) \leqslant 1.608\pi \qquad\qquad 2d_r(1 + |\sin \phi_1|) \leqslant 1.608\pi$$

To steer a null in the direction ϕ_0

$$\pi = 4d_r\sin\phi_0 + \delta_{2a}$$
$$\delta_{2a} = -4d_r\sin\phi_0 + \pi$$

$$\pi = d_r\sin\phi_0 + \delta_{2b}$$
$$\delta_{2b} = -d_r\sin\phi_0 + \pi$$

The delay required to produce the null consists of a fixed part (equal to the propagation path delay difference) plus a half-cycle of the frequency in question. Thus the setting of the array in this mode is frequency-dependent unless a combination of delay lines and phase inverters is used.

Substituting,

$$\psi_{2a} = 4d_r(\sin\phi - \sin\phi_0) + \pi$$

$$\psi_{2b} = d_r(\sin\phi - \sin\phi_0) + \pi$$

In the wanted direction

$$E_a(\phi = \phi_1) = E_{4a}(\phi = \phi_1)E_{2a}(\phi = \phi_1)$$
$$= 4 \,.\, 2\cos(\psi_{2a}/2)\ (\phi = \phi_1)$$

$$E_b(\phi = \phi_1) = E_{4b}(\phi = \phi_1)E_{2b}(\phi = \phi_1)$$
$$= 4 \,.\, 2\cos(\psi_{2b}/2)\ (\phi = \phi_1)$$

Compare

$$E_8(\phi = \phi_1) = 8$$

Thus the relative sensitivity in the wanted direction with the null in operation is

$$|\cos(\psi_{2a}/2)\ (\phi = \phi_1)|$$

$$|\cos(\psi_{2b}/2)\ (\phi = \phi_1)|$$

We have chosen to restrict this to ≥ 0.5 to prevent gross distortion of the main beam. So the second condition for the success of the configuration is

$$|4d_r(\sin\phi_1 - \sin\phi_0) + \pi| \leq \frac{2\pi}{3},$$

$$\text{or } \frac{4\pi}{3} \leq |\quad \ldots \ldots \quad| \leq \frac{8\pi}{3}, etc.$$

$$|d_r(\sin\phi_1 - \sin\phi_0) + \pi| \leq \frac{2\pi}{3},$$

$$\text{or } \frac{4\pi}{3} \leq |\quad \ldots \ldots \quad| \leq \frac{8\pi}{3}, etc.$$

It can be seen that the loss of sensitivity comes only from the "array of arrays" pattern. If the four-element pattern was steered slightly away from the wanted direction, there would be a further loss of sensitivity. Thus, considering the pattern of Fig. 4, the fact that the maximum of the pattern is not exactly in the wanted direction is unlikely to be a disadvantage, because no other setting of the array in this mode would give greater sensitivity in the wanted direction (given that a broadside null is required).

The fall-back strategy involves a small displacement of the steerable main beam pattern, such that one of the nulls falls in the direction ϕ_0.

The nulls in E_8 occur when

$$\psi = \pm l\frac{\pi}{4}, l = 1, 2, 3, \ldots$$

with the values $\psi = \pm 2k\pi$, when maxima occur, excluded

With the main beam steered in the direction ϕ_1

$$\psi(\phi) = d_r(\sin\phi - \sin\phi_1)$$

Then considering the direction ϕ_0

$$\psi(\phi = \phi_0) = d_r(\sin\phi_0 - \sin\phi_1)$$

By a suitable choice of Δ where $-\pi/8 \leq \Delta \leq \pi/8$ we can obtain

$$\psi_{null}(\phi = \phi_0) = d_r(\sin\phi_0 - \sin\phi_1) + \Delta = \pm l\frac{\pi}{4}$$

provided that $|\psi(\phi = \phi_0)| \geq \frac{\pi}{8}$

Then the requisite setting of the combining unit is

$$\delta_{null} = -d_r\sin\phi_1 + \Delta$$

The phase parameter becomes

$$\psi_{null} = d_r(\sin\phi - \sin\phi_1) + \Delta$$

and the pattern becomes

$$E_{null} = \frac{\sin(8\psi_{null}/2)}{\sin(\psi_{null}/2)}$$

In the wanted direction

$$\psi_{null}(\phi = \phi_1) = \Delta$$

$$E_{null}(\phi = \phi_1) = \frac{\sin(8\Delta/2)}{\sin(\Delta/2)}$$

The smallest value of $E_{null}(\phi = \phi_1)$ which we allow occurs when $\Delta = \pm\pi/8$ and is

$$\frac{\sin\pi/2}{\sin\pi/16} \simeq 5.1, \text{ compare } E_8(\phi = \phi_1) = 8$$

The fall-back scheme is treated as such because for a fixed null direction there is a very restricted set of directions in which the maximum can go, and only coarse direction finding of the wanted signal is then possible.

APPENDIX 2: ALTERNATIVE PROCEDURE FOR NULL STEERING

The method may be explained by reference to Fig. 25. To simplify the explanation, we assume that the wanted signal is in the broadside direction, but the method also applies to other directions. The top line of Fig. 25 shows eight vectors representing the complex (amplitude and phase) weighting applied to the element signals to put the main beam in the broadside direction. The weights are of equal amplitude and in-phase.

The next line of Fig. 25 shows the weights for a beam of low amplitude; this beam has been steered away from broadside by applying a linear phase slope across the array. The phases have been chosen so that the beam is in phase with the main beam. The weights for a second low-amplitude beam are given at (c). This beam has the same amplitude as the last. It has been steered symmetrically to the opposite side of the main beam and is 180° out-of-phase with the main beam. The direction of this second beam is the direction in which the null will be obtained. The amplitude of the two beams is set so that their combined pattern is equal in amplitude to
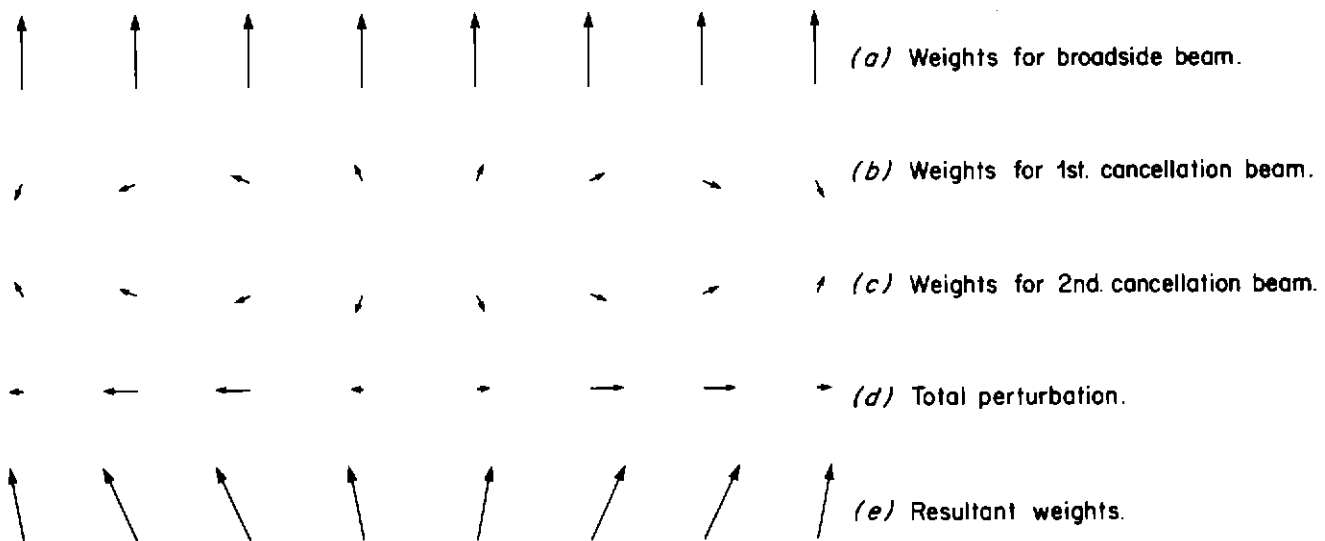

(a) Weights for broadside beam.

(b) Weights for 1st. cancellation beam.

(c) Weights for 2nd. cancellation beam.

(d) Total perturbation.

(e) Resultant weights.

Fig. 25 – Element weights for alternative null steering procedure.

the broadside beam pattern in the null direction (and also in the symmetrically opposite direction). Fig. 25 (d) shows the resultant of (b) and (c): it is the actual perturbation which is applied to the original weights (a).

The result is a cancellation in the null direction. In the symmetrically opposite direction, the patterns reinforce and the level of the broadside beam pattern is raised by 6 dB. The resultant of the perturbation and the original weights is shown in the bottom line of Fig. 25. Because the perturbations are in quadrature to the original weights, the resultants can be obtained, to a first-order approximation, by small adjustments to the original phases. It is necessary to have both the low-amplitude beams in order that the perturbations will be in quadrature, and thus be obtainable as described.

The procedure can readily be extended to steering more than one null. However, a pair of nulls cannot be placed symmetrically about the main beam.

As mentioned above, if the null direction is at the peak of a sidelobe of the initial pattern, the symmetrically opposite sidelobe is raised by 6 dB. It may therefore be desirable to reduce the level of some of the sidelobes in the initial pattern. Fortunately this null-steering procedure also works if the array has a symmetrical amplitude taper. For the present array, a Dolph-Chebyshev amplitude distribution could be used. This may be implemented with a small number of fixed attenuators in the combining unit. A suitable compromise for the sidelobe level would be in the range -17 dB to -20 dB, and the width of the main beam (between nulls) would be increased by between 10 and 20 per cent.